Asia-Pacific Journal of Atmospheric Sciences (2021) 57:573–585
https://doi.org/10.1007/s13143-020-00214-1

Online ISSN 1976-7951
Print ISSN 1976-7633

ORIGINAL ARTICLE

Diurnal Characteristics of Summer Precipitation Over Luzon Island, Philippines

Miguel Ricardo A. Hilario [1,2] · Lyndon Mark Olaguera [1,3,4] · Gemma Teresa Narisma [1,4] · Jun Matsumoto [3,5]

Received: 6 December 2019 / Revised: 28 June 2020 / Accepted: 20 July 2020 / Published online: 12 August 2020

Abstract

A network of 411 ground stations across Luzon Island, Philippines (12.5–20° N, 119–126.5° E) was used to characterize the diurnal cycles of summer precipitation, in terms of amount (PA), frequency (PF), and intensity (PI), during the southwest monsoon season (SWM; May–September) between 2011 and 2018. In addition to monsoon exposure, the effect of topography on the diurnal cycle of precipitation also was investigated by comparing a valley, plain, west- and east-facing coasts near mountains. Results show that monsoon exposure significantly influenced diurnal precipitation such that PA and PF decreased (PI increased) toward the leeward side of Luzon Island. Most topographies showed late afternoon-early evening peaks; however, the east-facing coast exhibited a late night-early morning peak. Orographic effects led to a high PA over mountains and enhanced the spatiotemporal propagation of PA in monsoon-exposed areas. The first (second) half of the diurnal peak exhibited high PI/low PF (low PI/high PF), suggesting both PI and PF are important indicators of PA. Finally, graded analysis revealed that light precipitation (0.01–2.5 mm h^{-1}) captured overall precipitation trends across Luzon Island, highlighting the importance of this intensity of precipitation. Heavy precipitation (2.5–7.5 mm h^{-1}) peaked in the morning; however, underlying mechanisms remain unknown. The study presents the first examination of the diurnal precipitation cycle in Luzon Island using a dense network of synoptic stations. The study demonstrates the complex effect of topography on precipitation and the importance of the SWM in the diurnal cycle of precipitation.

Keywords Philippines · Diurnal precipitation · Summer precipitation · Monsoons · Topography · Precipitation amount · Precipitation frequency · Precipitation intensity

1 Introduction

As the diurnal cycle of precipitation is an important component of regional climate, understanding the mechanisms behind precipitation formation is essential not only for the characterization of climate but also for the evaluation of satellite datasets and the improvement of the simulation and forecasting abilities of numerical models (Yang and Slingo 2001; Betts and Jakob 2002; Dai et al. 2007; DeMott et al. 2007; Jamandre and Narisma 2013). Furthermore,

Responsible Editor: Edvin Aldrian, Ph.D..

Electronic supplementary material The online version of this article (https://doi.org/10.1007/s13143-020-00214-1) contains supplementary material, which is available to authorized users.

✉ Lyndon Mark Olaguera
lmolaguera@observatory.ph

[1] Department of Physics, Ateneo de Manila University, Loyola Heights, 1108 Quezon City, Philippines

[2] Air Quality Dynamics Laboratory, Manila Observatory, Ateneo de Manila University campus, Loyola Heights, 1108 Quezon City, Philippines

[3] Department of Geography, Tokyo Metropolitan University, 1-1 Minami-Osawa, Hachioji-Shi, Tokyo 192-0397, Japan

[4] Regional Climate Systems Laboratory, Manila Observatory, Ateneo de Manila University campus, Loyola Heights, 1108 Quezon City, Philippines

[5] Dynamic Coupling of Ocean-Atmosphere-Land Research Program, Japan Agency for Marine Earth Science and Technology, 2-15, Natsushima-Cho, Yokosuka-Shi, Kanagawa 237-0061, Japan

precipitation amount (PA), frequency (PF), and intensity (PI) are important factors in determining several environmental quantities such as soil moisture variations, evaporation and runoff levels, and sensible heat flux over land (Qian et al. 2006; Takahashi and Polcher 2019). As such, the characterization of precipitation is needed to develop our understanding of regional climate variability as well as other environmental variables.

Characterization of precipitation is an extensively studied topic in climate research (Dai 2001a, 2001b; Trenberth et al. 2003; Sun et al. 2006, 2007; Dai et al. 2007; Zhang et al. 2017). It is well known that afternoon peaks in precipitation are characteristic of inland regions, while coastal regions typically exhibit late night-early morning peaks (Johnson 2011). Different precipitation intensities in the tropics show distinct diurnal peaks; showery precipitation tends to peak in the early morning and thunderstorms tend to occur around midnight, while diurnal peaks of drizzle and non-showery precipitation occur in the morning, particularly over land areas (Dai 2001). As differing intensities of precipitation vary in terms of their diurnal cycles, it is important to account for this when assessing precipitation characteristics (Hirose 2005; Zhuo et al. 2014). Topography also plays a major role in the local-scale precipitation patterns (Zhang et al. 2017). Peninsular regions such as Malaysia show coast-specific patterns of precipitation based on the prevailing monsoonal winds (Oki and Musiake 1994). Mountain ranges have also been shown to act as moisture barriers, thereby affecting precipitation levels on the leeward and windward sides of mountains (Xie et al. 2006). Similarly, numerical simulations have shown that land-sea breeze, orographic uplifting, and the horizontal scale of islands over the Maritime Continent (MC) are important in determining the timing of convective intensity (Saito et al. 2001). Furthermore, numerical simulations of precipitation in the South China Sea found that both local- and large-scale circulation must be accounted for to properly model the peak timing of diurnal precipitation (Park et al. 2011). Local-scale convection in the form of mountain-valley breeze and land-sea breeze are important considerations in determining peak precipitation timing (Ohsawa et al. 2001). Similarly, large-scale monsoonal circulation plays an important role in the seasonal moderation of the diurnal precipitation cycle (Qian et al. 2010; Yuan et al. 2010).

In tropical and subtropical Asia, precipitation characteristics has been extensively studied in the Indochina Peninsula (Satomura 2000; Ohsawa et al. 2001; Yokoi et al. 2007; Takahashi 2010, 2016; Tsujimoto et al. 2018; Takahashi and Polcher 2019), Malaysia (Oki and Musiake 1994), Indonesia (Mori et al. 2004; Sakurai et al. 2005, 2009, 2011; Shibagaki et al. 2006; Qian 2008; Qian et al. 2010; Yamanaka 2016; Yamanaka et al. 2018), and East Asia (Fujibe 1999; Zhou et al. 2008; Yin et al. 2009; Yuan et al. 2010; Zhuo et al. 2014); however, although previous studies have addressed long-term, seasonal, and sub-seasonal precipitation trends in the Philippines (Akasaka et al. 2007; Cruz et al. 2013; Villafuerte et al. 2014; Olaguera et al. 2018a, 2018b), little attention has been paid to characterizing the diurnal precipitation cycle. The Philippines (5–25° N, 115–135° E) is an archipelago located in the western Pacific, east of the South China Sea. As shown in Fig. 1a, the Philippines is composed of two major islands in the north and south: Luzon and Mindanao, respectively and a central cluster of smaller islands: Visayas. The Philippines is topographically diverse, characterized by mountain ranges, plains, valleys in relative proximity, and surrounded by coasts through which the country is exposed to large-scale monsoonal winds (Coronas 1920; Flores and Balagot 1969; Matsumoto et al. 2020). Previous precipitation studies divided areas of interest into sub regions to identify the effect of terrain distribution on the diurnal cycle of precipitation (Yu et al. 2007; Zhou et al. 2008, 2014). In this study, we focus on four regions in the northern major island of Luzon as case studies of the effect of topography and monsoonal influence on the diurnal cycle of precipitation, due to the exposure to the monsoonal influence and the presence of key topographical features. These four regions are shown in Fig. 1b and include: the Central Luzon Plain (CLP; 15–16.15° N, 120.5–121.2° E), the West Luzon Coast (WLC; 15–18.5° N, 119.7–120.55° E), the East Luzon Coast (ELC; 14.6–16.5° N, 121.3–122.5° E), and Cagayan Valley (CV; 16.5–18° N, 121.4–122° E). These areas were chosen due to their distinct topography and location relative to monsoonal winds.

As the monsoons are integral components of the Philippine climate, one focus of our analysis is the influence of monsoon exposure on the diurnal precipitation profile of a region. Large-scale meteorological phenomena such as seasonal monsoons are of particular importance when characterizing precipitation in a region such as the Philippines, which is situated near the Asian monsoonal trough (Akasaka et al. 2007). The Philippines experiences wet and dry seasons depending on the prevailing influence of the southwest (SWM; May to September, MJJAS) and northeast monsoon (NEM; November to March, NDJFM) seasons (Matsumoto et al. 2020). The months of October and April act as transition periods between the SWM and NEM (Moron et al. 2009; Akasaka 2010; Olaguera and Matsumoto 2019; Matsumoto et al. 2020). Monsoon transition is nonhomogeneous such that onset and withdrawal do not occur uniformly across the Philippines. For example, it was observed that NEM onset begins in the northern regions of the Philippines moving southwards (Kubota et al. 2017). The annual progression of the monsoon is a result of several changes in large-scale circulation. The seasonal march of precipitation is marked by sudden changes in circulation, particularly the eastward shift in the subtropical high, deepening of the monsoon trough east of the Philippines, and the retreat of the easterlies (Akasaka

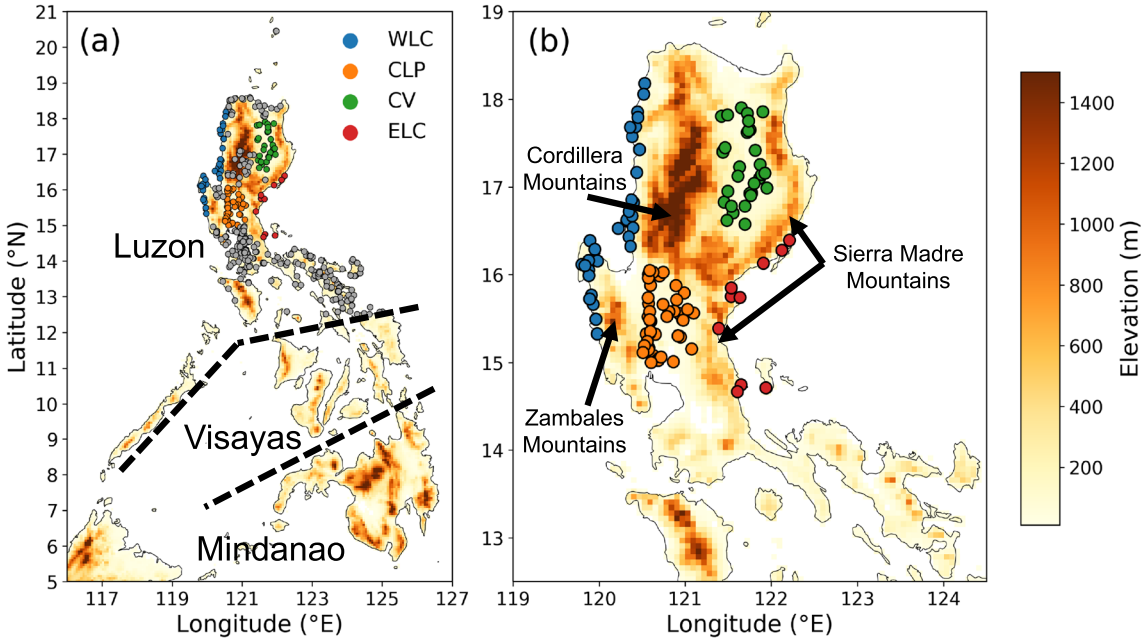

Fig. 1 **a** Elevations (m) and locations of all stations used in this study, and **b** enlarged map of northern Luzon Island showing only stations in West Luzon Coast (WLC, blue), Central Luzon Plain (CLP, orange), Cagayan Valley (CV, green), and East Luzon Coast (ELC, red). Major islands of the Philippines are divided by dashed lines in (**a**) and major mountain ranges are labelled in (**b**). Elevation color bar and station symbols are for both (**a**) and (**b**)

et al. 2007). Akasaka et al. (2007) and Matsumoto et al. (2020) noted a sharp contrast between the seasonal march on the west and east coasts of the Philippines: the west coast shows its rainy season in the summer while the east coast experiences its rainy season in the winter. While the mountain ranges along the western and eastern side of the Philippines (Cordillera and Zambales mountain ranges on the west and Sierra Madre mountain range on the east, respectively as shown in Fig. 1b) contribute to the spatial contrast of precipitation by creating drier conditions on the leeward sides of the mountains relative to the prevailing winds (Qian 2008), the changes in the prevailing large-scale monsoon system primarily influence the distribution of rainfall. During MJJAS, for example, the western (eastern) coast experiences its (dry) rainy season. The opposite occurs during NDJFM. Therefore, we expect the diurnal precipitation cycle of the Philippines to be a combination of local- and large-scale monsoonal influences, which is characteristic of island regions (Chang et al. 2005; Akasaka et al. 2007; Xin-Xin et al. 2015).

Often in regions that lack high resolution observation datasets, high resolution regional climate models and land surface models are needed to study variability in the water cycle and to produce seasonal climate predictions (Qian et al. 2006); however once high-resolution observation datasets exist, it is important for these model-based studies to be validated using observation datasets. Previous precipitation studies on the Philippines utilized a limited number of meteorological stations from the Philippine Atmospheric, Geophysical and Astronomical Services Administration (PAGASA), and most of these studies used a maximum of 59 operational stations distributed over the Philippines (Akasaka et al. 2007; Jamandre and Narisma 2013; Villafuerte et al. 2014). Additionally, these studies did not focus on the diurnal cycle of precipitation or the characterization of the diurnal cycle at different precipitation intensities, since almost no observation data have been available in a sub-daily time scale. With the lower spatiotemporal resolution used in previous ground-based studies and the need to validate studies using satellite data, the novel network of 411 meteorological stations across Luzon Island offers an opportunity to characterize precipitation in the Philippines at a much higher spatial and temporal resolution. In this study, we focus on Luzon Island to highlight the influence of topography on the diurnal cycle. Furthermore, we narrow the scope of the study to MJJAS due to the role of the SWM as it contributes the majority of precipitation throughout the year in most of the target region. Given the diverse topography types and influence of the SWM, we ask: how do the diurnal cycles of PA, PF, PI respond spatially through different topography types considering the influence of the SWM?

The objectives of this study are, therefore, to (1) describe the spatial patterns of the diurnal cycle of precipitation over the Philippines including PA, PF, and PI; and (2) identify regional differences (i.e., topography or location) in the diurnal cycle of precipitation in relation to the SWM. The rest of the paper is organized as follows. Section 2 provides a description of the datasets and methodology used in this study. The regional characteristics of the diurnal cycle of

precipitation are examined in Section 3. A summary and discussion are provided in Section 4.

2 Data and Methodology

2.1 Data

A ground-based, high spatiotemporal-resolution dataset of 411 stations in Luzon Island by the Weather Philippines Foundation (WPF; https://weatherph.org) spanning between January 2011 and April 2018 was used in this study to describe the diurnal variations of precipitation in Luzon Island. Previous studies have shown that several years of data spanning less than a decade is sufficient to obtain a stable diurnal cycle (Dai et al. 2007; Zhou et al. 2008). The dataset was collected at a 10 min resolution and includes several meteorological variables such as precipitation amount, 2-m temperature, dew point, wind speed, wind direction, and incident solar radiation. The minimum threshold of precipitation measured by the stations is 0.2 mm in 10 min. The data were converted into hourly resolution to obtain accumulated hourly precipitation.

To further examine the mechanisms behind the observed diurnal precipitation cycle, data on 3-hourly 925 mb divergence and wind vectors for MJJAS between January 2011–April 2018 were obtained from the European Centre for Medium-range Weather Forecasts (ECMWF) reanalysis ERA5 (0.25° × 0.25°) via the Copernicus Climate Change Service (https://cds.climate.copernicus.eu) (Hersbach et al. 2019).

2.2 Methodology

Station data were filtered via completeness test per station, which removed months with more than 20% of precipitation data missing. We removed days when a tropical cyclone (TC; wind speed >17 m s^{-1}) is located within the Philippine Area of Responsibility (PAR; bounded by the following six coordinates: 120° E, 25° N; 135° E, 25° N; 135° E, 5° N; 115° E, 5° N; 115° E, 15° N; 120° E, 21° N; see Fig. 6 of Matsumoto et al. 2020) – hereafter termed TC days, in order to avoid their pronounced non-diurnal precipitation. As a consequence, about 18–35% of the data were removed from the stations during the peak TC season in MJJAS. No station had a missing month after this filtering of TC days. During the study period, 365 days were classified as TC days and were removed from the dataset. It is also worth mentioning that the precise influence of the monsoon is difficult to isolate in this study. Therefore, precipitation is expected to be a combination of the diurnal cycle and the effect of the prevailing monsoon.

The precipitation data from the stations were interpolated onto regular grid points with a horizontal resolution of 0.15° × 0.15° (~17 km × 17 km). Interpolation was performed through inverse distance weighting (IDW) that employs proximity-weighted interpolation, which means that considering a neighborhood of points, nearer values are given more importance than farther values when interpolating. The IDW algorithm is described more fully in Chen and Liu (2012). We focus our analysis only on the MJJAS season, but we note here that the spatial trends for NDJFM are largely opposite to those of MJJAS, which may be explained by the opposite direction of prevailing wind (Akasaka et al. 2007). Spatial trends for April resemble an intermediate between the two seasons, a characteristic of a transition period. Following Zhang et al. (2017), for each hour in a day, PA is defined as the climatological average of accumulated hourly precipitation divided by the total number of hours within the season, PF is defined as the total number of hours with hourly-averaged precipitation above 0.01 mm $hr.^{-1}$ divided by the total number of hours in the season, and PI is defined as PA divided by PF (PI=PA/PF). We note that the total number of hours within the season excludes hours with missing data.

As mentioned in Section 1, we divide Luzon Island into four regions to further depict the regional differences in the diurnal cycle of precipitation. These four regions are shown in Fig. 1b and include the CLP (46 stations), the WLC (36 stations), the ELC (10 stations), and the CV (32 stations). We note that weather stations located on mountain ranges (Fig. 1b) have poor data completeness and were not included in the comparison of topography types.

3 Characteristics of PA, PF, and PI

3.1 Seasonal Changes in PPA, PPI, PPF

3.1.1 Peak Precipitation Amount

Figure 2 shows the peak PA/PF/PI (hereafter, PPA/PPF/PPI) throughout Luzon for the SWM period in MJJAS. The Philippines in MJJAS (Fig. 2a) exhibits high PPA values above 1.0 mm h^{-1} along the WLC due to the Cordillera mountains (Fig. 1b), indicating orographic effects on precipitation amount as observed in other studies (Ohsawa et al. 2001; Xie et al. 2006; Minamide and Yoshimura 2014) associated with heat balance along the mountain slope (Reiter and Tang, 1984). The presence of the mountain ranges creates a remarkably clear delineation between leeward (PPA < 0.8 mm h^{-1}) and windward (PPA > 1.0 mm h^{-1}) sides, similar to other studies (Akasaka et al. 2007; Zhuo et al. 2014; Pullen et al. 2015; Takahashi 2016). Over the ELC, PPA appears to be relatively less compared to the WLC. Figure S1 of the Supplementary Information (SI) depicts the timing of PPA/PPF/PPI. Most of Luzon Island exhibits PPA in the late afternoon (Fig. S1**a**), indicating the effect of solar heating on the diurnal cycle. An exception to the late afternoon occurrence of

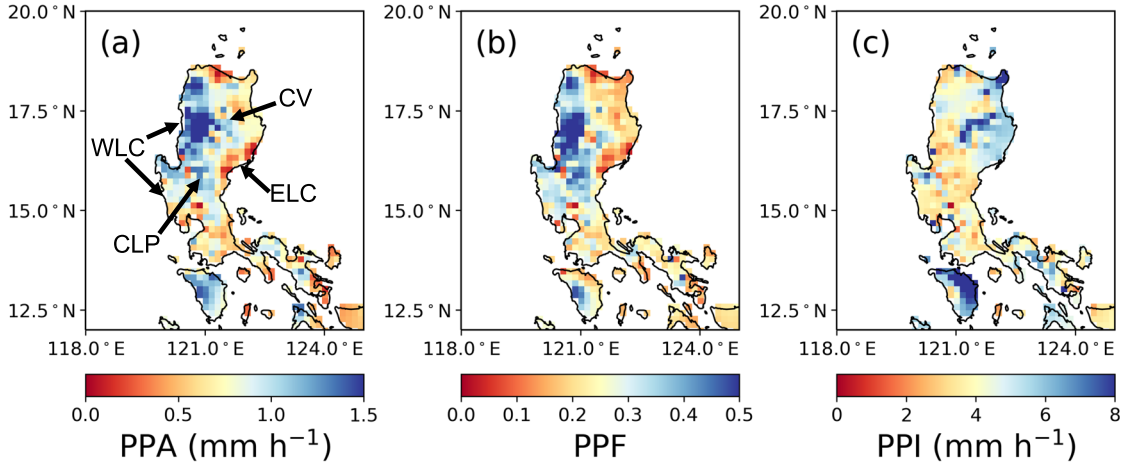

Fig. 2 **a** Peak precipitation amount (PPA; mm h^{-1}), **b** frequency (PPF), and (**c**) intensity (PPI; mm h^{-1}) for the southwest monsoon season (MJJAS). Regions are labelled in (**a**)

PPA is seen over the ELC, which shows PPA between late evening and early morning (23–3 LST).

3.1.2 Peak Precipitation Frequency

As shown in Fig. 2b, PPF in Luzon shows a similar spatial distribution as PPA, which suggests that total precipitation amount is largely dependent on the frequency of precipitation. Heightened PPF above 0.4 is observed along the WLC, CLP, and the Cordillera mountains while lower PPF below 0.3 are observable in the CV and ELC. Spatially, PPF in MJJAS generally decreases from west to east, corresponding to monsoon flows. The strong relationship between PA and PF has also been observed in other coastal regions (e.g., Zhuo et al. 2014). Such a connection is also observable in the similar timings of PPF and PPA (Fig. S1a–b).

3.1.3 Peak Precipitation Intensity

Luzon Island shows a spatial distribution of PPI (Fig. 2c) that is distinctive from PPA and PPF (Fig. 2a–b). Figure 2c reveals high PPI (>6.0 mm h^{-1}) over the CV and along the northeast coast of Luzon, and low PPI (<4.0 mm h^{-1}) over the CLP and most of the WLC. The late afternoon occurrence of PPI (Fig. S1c) (18–21 LST) over the CLP and the CV generally agrees with the timing of PPA and PPF (Fig. S1a–b). Over the ELC, PPI (18–22 LST) occurs in advance of PPA and PPF. Interestingly, parts of the WLC exhibit PPI in the morning (6–12 LST), in contrast to the timings of PPA and PPF in the late afternoon (Fig. S1a–b). This feature is further examined in Sections 3.5 and 4.

3.2 Seasonal-Diurnal Profiles of Selected Regions

Seasonal-diurnal plots of PA (Fig. 3) show the time evolution of the diurnal cycle throughout the year. In general, the annual peak of PA occurs in MJJAS with the exception of ELC, which has its annual PA peak in December (Fig. 3d)—a difference attributable primarily to monsoon influence and to a lesser degree heterogeneous topography. In the WLC (Fig. 3a) and CLP (Fig. 3b), high PA values (>0.6 mm h^{-1}) are seen from June to August during the peak of the SWM. while moderate PA values (0.2–0.6 mm h^{-1}) are seen in May and September. The diurnal peaks of PA (>0.6 mm h^{-1}) in the WLC and CLP occur between 15 LST and 20 LST, with WLC exhibiting noticeably higher PA throughout the day. As the WLC is located on the windward side of the Philippines relative to the prevailing SWM winds in MJJAS, the Cordillera mountains to the east most likely enhance PA (Fig. 1b). The CLP exhibits heightened PA in MJJAS, which is attributable to SWM influence as well as orographic effects from the nearby Cordillera and Sierra Madre mountain ranges (Fig. 1b). In contrast, the Zambales mountains to the west of the CLP (Fig. 1b) may induce a rain shadow effect over the western side of the CLP, lowering PA. Such spatial effects are further discussed in Section 3.4.

In July and August, the WLC exhibits higher PA throughout the day than the CLP, which may be due to the more direct exposure of the WLC to the southwesterly monsoon. The different timings of precipitation in the WLC may be explained by different mechanisms such as daytime convection induced by differential heating over land (Park et al. 2011) and evening land breeze converging with large-scale monsoonal winds (Ohsawa et al. 2001), which are further discussed in Section 3.6. The WLC and CLP show low PA during other times of the year, suggesting that PA in these two regions is regulated by the orientation of the nearby mountain ranges to the seasonal monsoons (Fig. 1b), typical of insular regions in Asia (Chang et al. 2005).

Compared to the CLP and WLC, the CV (Fig. 3c) shows a longer seasonal peak of PA from May to September and a slightly narrower diurnal peak between 17 LST and 20 LST.

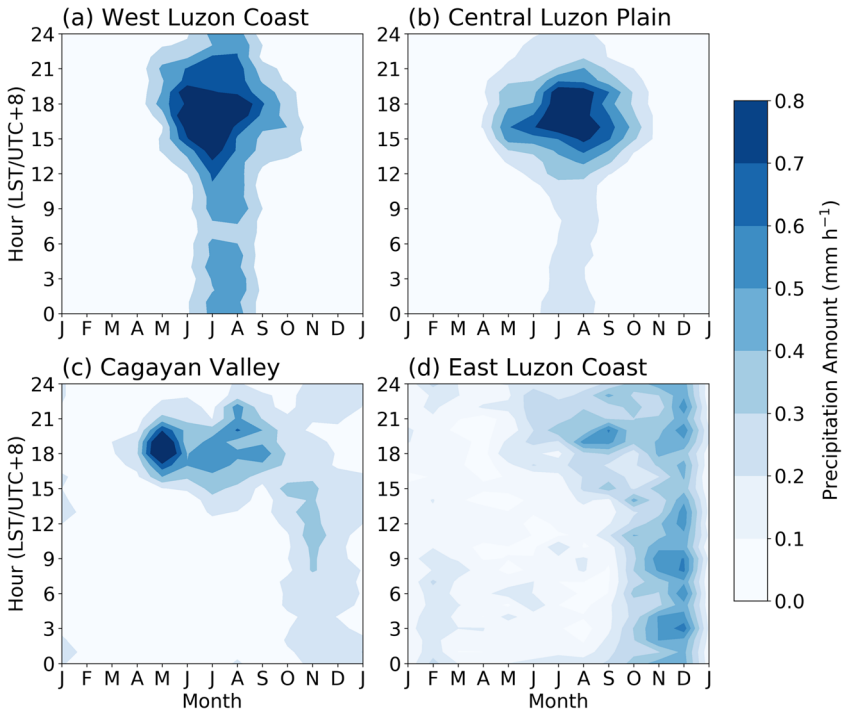

Fig. 3 Seasonal-diurnal profiles of precipitation amount (in units of mm h^{-1}) for (**a**) West Luzon Coast (WLC), (**b**) Central Luzon Plain (CLP), (**c**) Cagayan Valley (CV), and (**d**) East Luzon Coast (ELC)

The CV region shows its clearest diurnal cycle in May, with a peak PA value exceeding 0.8 mm h^{-1} from 17 to 20 LST. Furthermore, the diurnal peak of PA in the CV between June and August reaches 0.5 mm h^{-1}. This is not as high as the PA peak in the CLP and WLC, which suggests the Cordillera mountain range west of the CV (Fig. 1b) plays a role in dampening the influence of the SWM. Interestingly, we observe a shift in the diurnal peak between September and December towards earlier times of the day, perhaps related to the transition of the SWM to the NEM.

In contrast to the usual peak in MJJAS in other regions, the ELC (Fig. 3d) shows an annual PA maximum of around 0.5 mm h^{-1} in December with near-constant precipitation throughout its diurnal cycle. This characteristic was also observed by Akasaka et al. (2007), who noted that precipitation in the ELC peaks in December and is more strongly influenced by the NEM than the SWM. Aside from the PA maximum in December, we observe a secondary maximum in August–September of 0.4 mm h^{-1} that occurs around 20 LST. This is likely related to a combination of sea breeze and solar heating over the mountains to the west. This peak shifts from early evening in August (20 LST) to early morning in December (3 LST), suggesting that it is a function of the SWM and NEM.

3.3 Diurnal Profiles of Selected Regions

The PPA/PPI/PPF maps (Fig. 2) and seasonal-diurnal plots (Fig. 3) reveal distinct diurnal cycles across different regions as a function of local topography and the seasonal monsoon. To further elucidate these differences, Fig. 4 shows the diurnal cycle in terms of PA/PI/PF at the four selected regions for MJJAS.

3.3.1 Precipitation Amount

Figure 4a shows the diurnal cycle of PA across the four regions. MJJAS is characterized by the highest PA, exceeding 0.8 mm h^{-1} in the WLC, 0.6 mm h^{-1} in the CLP, 0.5 mm h^{-1} in the CV, and 0.25 mm h^{-1} in the ELC (Fig. 4a). These values are significantly higher than those in other months (not shown). The PA values in MJJAS represent the annual maximum in all four regions except for ELC. Diurnal peak timings differ among regions, occurring first in the CLP (16 LST), followed by the WLC (17 LST), then the CV (18 LST), and finally the ELC (20 LST). Similar late afternoon-early evening precipitation peaks have been observed in other insular regions (Takahashi 2010; Xin-Xin et al. 2015) and reflect the large-scale monsoon influence (Zhuo et al. 2014). We note that the slightly delayed PA peak in the ELC may be due to the presence of the southern Sierra Madre mountains suppressing SWM flows (Fig. 1b).

3.3.2 Precipitation Frequency

The diurnal cycle and seasonal profiles of PF (Fig. 4b) track those of PA (Fig. 4a) quite well across regions, suggesting that PF is an important factor for PA. PF is the highest in MJJAS for all regions (0.3 in the WLC and CLP, 0.2 in the CV) except the ELC, which peaks in NDJFM (not shown). Interestingly, the ELC shows relatively low diurnal variability in PF (0.8–

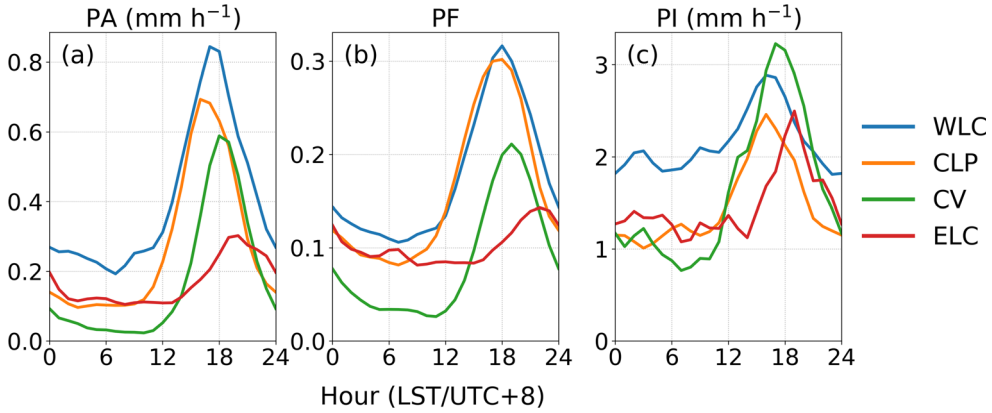

Fig. 4 Diurnal variations of (**a**) precipitation amount (PA; in units of mm h^{-1}), (**b**) frequency (PF), and (**c**) intensity (PI; in units of mm mm h^{-1}) for West Luzon Coast (WLC; blue), Central Luzon Plain (CLP; orange), Cagayan Valley (CV; green), and East Luzon Coast (ELC; red) for the southwest monsoon season (MJJAS). Values were smoothened with a 3-hourly running mean

1.3) in MJJAS, indicative of sustained precipitation throughout the day. This feature may be explained by the combination of daytime mountain and sea breeze producing stronger upslope flow along the Sierra Madre mountains (Fig. 1b) and the combination of nighttime land and mountain breeze leading to convergence due to the concave curve of the ELC (i.e., sea extending landward). Such mechanisms are known to influence precipitation over the coastal regions near mountains (Biasutti et al. 2012), discussed further in Section 3.6.

3.3.3 Precipitation Intensity

The diurnal cycle of PI (Fig. 4c) reveals a general increase throughout the day, indicative of local convective activities (Zhuo et al. 2014). Peaks in PI occur in the late afternoon (16–17 LST) in the WLC, CV, and CLP, and early evening (19 LST) in the ELC. All regions exhibit PI peaks exceeding 2.0 mm h^{-1} in MJJAS, with the highest PI occurring over the WLC (16–17 LST) and CV (17 LST). These coincident diurnal peaks across regions are indicative of the large-scale influence of the SWM over Luzon in MJJAS, as such homogeneity in the diurnal cycle was not observed in other seasons (not shown).

The similarity among the timings of diurnal peaks in PA, PF, and PI suggests that PF and PI are both important factors for the total PA. We note that in general PI (PF) peaks before (after) PA by 1–2 h. This reveals a shift in the characteristics of precipitation over the course of the diurnal PA peak, with the first (second) half exhibiting high PI and low PF (low PI and high PF). It is also noted that peak PI is highest in the CV followed by the WLC, while lower PI are observed over the ELC and CLP.

3.4 Spatiotemporal Propagation of PA

The time-longitude plots are useful for showing the spatial propagation of precipitation over time. Figure 5 shows the time-longitude plots of PA in each region for MJJAS. In the WLC (Fig. 5a), multiple PA peaks (>0.4 mm h^{-1}) are observed west of 120.2° E at 9, 14, and 17 LST. One explanation for this longitudinal variation may be related to a more pronounced orographic effect from the Zambales mountains compared to the Cordilleras (Fig. 1b), the former (latter) of which is adjacent to the southwest (northeast) portion of the WLC. We note that the boundary between southwest and northeast WLC is denoted by a black arrow in Fig. 5a. The southwestern WLC located west of the Zambales mountains (119.7–120.2° E) shows multiple peaks over 0.6 mm h^{-1} at 9, 15, and 18–22 LST, indicative of different physical mechanisms. In comparison, the northeast WLC located west of the Cordilleras (120.2–120.55° E) shows a clear PA peak of over 0.6 mm h^{-1} between 17 and 18 LST. The PA peak over the WLC shows a slight eastward time delay, occurring first at around 14 LST over the southwestern WLC, propagating northeast and resulting in a peak at 18 LST across the whole WLC. The recession of nighttime PA exhibits a slight delay along the southwestern WLC, dropping at 21 LST first over the northeastern WLC (120.3–120.6° E) then past 23 LST over the southwestern WLC (119.7–120.3° E). The propagation of PA over the WLC is only visible in MJJAS and is not observed in other seasons (not shown), which is explainable by the weakening of large-scale circulation in other seasons by nearby mountain ranges (Xie et al. 2006).

The CLP (Fig. 5b) shows heightened PA values over 0.4 mm h^{-1} across the plain (120.5–121.2° E) beginning at 14 LST until 20 LST; however, the propagation of PA is not uniform. The onset of the peak begins as early as 12 LST, occurring first on the east and west edges of the CLP near the mountains (Fig. 1b) likely from convection induced by solar heating, but after 14 LST, higher PA values (>0.5 mm h^{-1}) are well-constrained to the eastern side of the CLP (120.9–121.2° E). During the recession of the diurnal PA peak, PA first drops along the western side of the CLP (120.5–120.8° E) below 0.4 mm h^{-1} as early as 17 LST, while the eastern side exhibits heightened PA lasting until 20 LST. The lower (higher) PA over the western (eastern) CLP is likely due to its location on the leeward (windward) side of the Zambales (southern Cordillera and Sierra Madre) mountain ranges relative to the prevailing SWM wind (Fig. 1b).

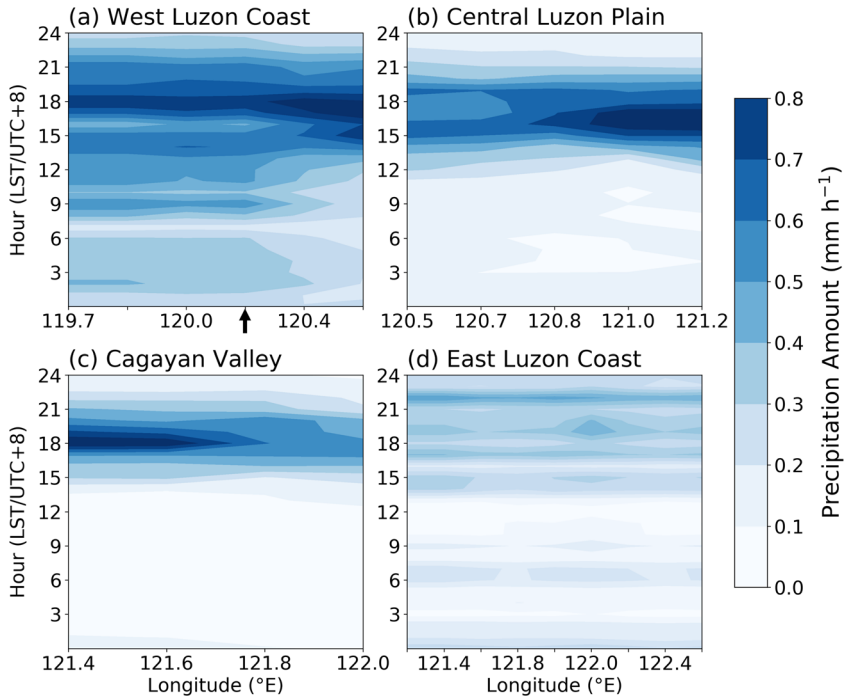

Fig. 5 Time-longitude cross sections of precipitation amount (PA; in units of mm h^{-1}) during the southwest monsoon season (MJJAS) for (**a**) West Luzon Coast (WLC), (**b**) Central Luzon Plain (CLP), (**c**) Cagayan Valley (CV), and (**d**) East Luzon Coast (ELC). The boundary between northern/eastern and southern/western WLC is indicated by an arrow along the x-axis of (a)

In MJJAS, the CV (Fig. 5c) shows a very sharp PA peak over 0.5 mm h^{-1} between 17 and 18 LST that is largely constrained to its western side (121.4–121.7° E) adjacent to Cordillera mountains, which is indicative of convection induced by slope heating or interactive effects of heat balance (Reiter and Tang 1984; Ohsawa et al. 2001; Xie et al. 2006; Takahashi 2010; Xin-Xin et al. 2015). The eastern CV exhibits a similar late afternoon peak in PA but at lower values, reaching 0.5 mm h^{-1} between 17 and 20 LST.

The ELC (Fig. 5d) in MJJAS shows region-wide PA peaks appearing between 14 LST and 22 LST, with the highest PA occurring at 22 LST. These peaks occur synchronously across the ELC, indicating uniform convection along the east coast, perhaps from land breeze (Qian 2008; Qian et al. 2010). The multiple peaks scattered throughout the day appears in other seasons as well (not shown), indicating that this feature is local in origin. One explanation is the migration of precipitation down mountain slopes in the afternoon and evening in combination with the concave curvature of the coast (i.e., sea extending landward) (Biasutti et al. 2012). These factors may also be responsible for the early evening PI peak (Fig. 4c) but the migration of precipitation is not visible in Fig. 5d due to the equal distances of the ELC stations from the Sierra Madre mountain range (Fig. 1b).

3.5 Diurnal Profiles of PA with Different Precipitation Intensities

The diurnal cycle has been shown to vary depending on the intensity of precipitation (Zhuo et al. 2014). To investigate diurnal cycles of different intensities, hourly precipitation was divided into grades: 0.01–2.5 mm h^{-1} (hereafter referred to as light precipitation), and 2.5–7.5 mm h^{-1} (heavy precipitation). PA was then calculated for each precipitation grade. Precipitation above 7.5 mm h^{-1} is not described as it was rarely observed due to the filtering of TC days. Figure 6 shows stacked bar graphs of the diurnal cycles of the WLC (blue), CLP (orange), CV (green), and ELC (red) by precipitation grade for MJJAS.

Across regions, MJJAS shows a very defined diurnal cycle, accumulating into a late afternoon-early evening peak (17–18 LST; 2.4 mm h^{-1}) for light precipitation (Fig. 6a) and a morning peak (8–9 LST; 12.5 mm h^{-1}) for heavy precipitation (Fig. 6b). Light precipitation is predominantly contributed by the WLC and CLP, as expected due to their SWM enhancement. Heavy precipitation in MJJAS is contributed largely by the WLC from 8 to 12 LST, while the ELC, CV, and CLP contribute to heavy precipitation only from 8 to 9 LST. The heavy precipitation observed in the WLC is perhaps a product of local effects as it is also observed for the NEM months (not shown). Heavy precipitation over the WLC likely contributes to the timing of PPI in the morning (Fig. S1c).

The graded PA analysis reveals that light precipitation is largely responsible for observed precipitation in Luzon. This is corroborated by the similarity of the diurnal cycles of total precipitation per region (Fig. 4) to the diurnal cycles of light precipitation (Fig. 6a). This finding has implications for the accuracy of satellite-based precipitation products, which have shown to exhibit biases under precipitation extremes (Jamandre and Narisma 2013; Maggioni et al. 2016;

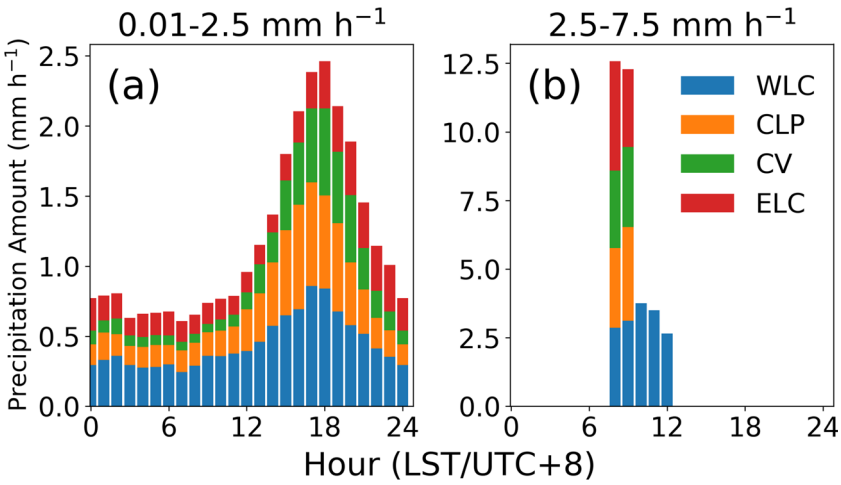

Fig. 6 Diurnal cycle of PA (mm h^{-1}) over the four regions, West Luzon Coast (WLC), Central Luzon Plain (CLP), Cagayan Valley (CV), and East Luzon Coast (ELC) for (**a**) 0.01–2.5 mm h^{-1} and (b) 2.5–7.5 mm h^{-1}

Mahmud et al. 2017). Furthermore, this underlines the need to better understand the behavior of precipitation in regions of complex topography in order to improve the performance of satellite-based precipitation products.

3.6 Low-Level Convergence and Winds

Figure 7 depicts ERA5 3-hourly 925 mb divergence and winds over Luzon Island averaged for MJJAS in terms of the diurnal anomaly, which is defined as the difference between the circulation features at the specified time and the daily mean. Figure S2 is similar to Fig. 7 but provides the circulation features in terms of the mean at the specified time. The diurnal cycle of divergence over the selected regions (Fig. S3) is directly comparable to the diurnal cycle of precipitation (Fig. 4). The diurnal cycle of PA is generally well-explained by low-level afternoon convergence (Figs. 7e–g, S2e–g, S3) over the CLP (17 LST), WLC (20 LST), CV (17 LST). Such convection is the result of late afternoon-early evening convection from solar heating throughout the day (Zhang et al. 2017). Additionally, southwesterly-westerly wind west of Luzon between 14 and 17 LST (Figs. 7e–f and S2e–f) in combination with orographic uplift may contribute to the remarkably high PA observed over the WLC (Fig. 4a). Convergence maxima over the Cordillera and Sierra Madre mountains highlight the importance of mountain ranges in determining the diurnal cycle of precipitation (Figs. 1 and 7). Consequently, the regions generally show late afternoon-early evening precipitation peaks (Fig. 4). In the case of the ELC, we observe a profile (Fig. S3) that somewhat

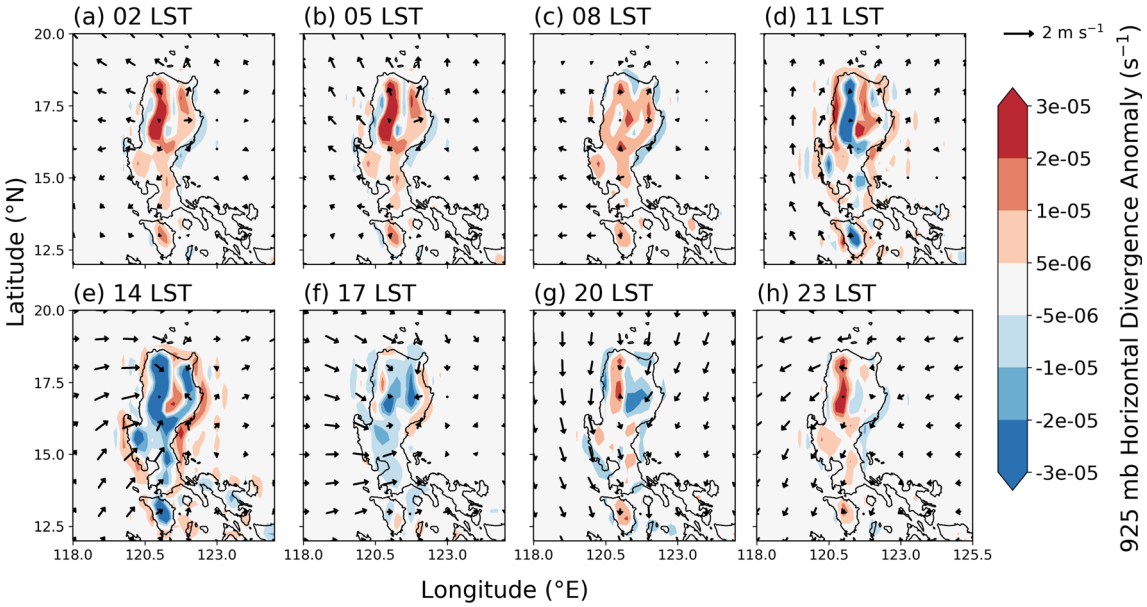

Fig. 7 Spatial distribution of ERA5 3-hourly 925 mb horizontal divergence (s^{-1}) and winds (m s^{-1}) in terms of the anomaly from the daily mean over Luzon Island averaged during the southwest monsoon season (MJJAS)

corresponds to the diurnal precipitation cycle (Figs. 4 and 5); however, the ELC experiences divergence throughout its diurnal cycle (Fig. S3) and thus the mechanism behind the scattered precipitation over the ELC remains a topic for future research. Furthermore, the effect of coastal curvature on diurnal winds is not visible and requires higher resolution modelling in future work. The potential migration of precipitation down mountain slopes (e.g., Biasutti et al. 2012) from the Cordillera mountain range to the WLC is also recommended as a topic of future research.

We note that mountain regions in Luzon island show early convergence maxima at 14 LST (Fig. 7), which is earlier than other parts of the island and precede precipitation peaks in adjacent regions. The slight difference in timing of the observed precipitation compared to the ERA5 convergence maxima may be explained by the time delay of migration down the mountain slopes. The calculation of accumulated precipitation also consequently creates a time delay between accumulated and real-time variables. Finally, the parameterization of the ERA5 reanalysis as a global output may lead to a bias in peak timing, as opposed to a locally parametrized model.

4 Discussion and Conclusions

4.1 Discussion

Precipitation in the Philippines has been shown to be a product of both local and large-scale circulation patterns (Park et al. 2011). Luzon is exposed to the SWM/NEM for majority of the year. Consequently, the diurnal cycle of precipitation over Luzon is largely a function of the interaction of different topographical features (valleys, mountains, coasts, plains) with the seasonal monsoons (Akasaka 2010; Cruz et al. 2013; Pullen et al. 2015; Riley Dellaripa et al. 2020). Diurnal and seasonal precipitation is further complicated by heterogeneous topography such as (1) mountain ranges, which serve as moisture barriers (Ohsawa et al. 2001; Xie et al. 2006) and produce strong vertical motion and subsequently heavy precipitation on windward sides (Cayanan et al. 2011), and (2) coasts, which serve as centers of interaction between local and large-scale circulation.

The interaction of topography and monsoon is most evident in the enhancement of all precipitation variables over Luzon Island, associated with the convergence of the prevailing SWM flow with nearby mountain ranges (Figs. 1 and 4). Our results corroborate the findings of Riley Dellaripa et al. (2020), which found topographic height to be a major factor in precipitation characteristics over the Philippines. During MJJAS, we observed generally late afternoon-early evening PA peaks (Fig. 4a) with slight differences in timing between regions: CLP (16 LST), WLC (17 LST), CV (18 LST), and ELC (20 LST). The generally late afternoon-early evening peaks have been observed in other insular regions across tropical Asia (Ohsawa et al. 2001; Takahashi 2010; Xin-Xin et al. 2015), and similarities in the diurnal cycle between regions, specifically the WLC and CLP, are indicative of the influence of large-scale circulation (Park et al. 2011; Zhuo et al. 2014). Indeed, the influence of the SWM is quite pronounced along the west coast of Luzon Island (Cruz et al. 2013) where mountains may contribute to clear diurnal peaks (Figs. 4 and 6) and the highest PA of the year for the WLC and CLP (Figs. 3 and 4) (Riley Dellaripa et al. 2020). Furthermore, the diurnal peak timing in MJJAS is generally well-explained by low-level convection induced by afternoon solar heating over the Cordillera mountains (Figs. 7 and S2). The combination of orographic effects from the Cordillera mountains and large-scale circulation from the SWM resulted in the spatiotemporal propagation of PA for regions that are exposed to the SWM such as the WLC and CLP (Fig. 5). The WLC and CLP are contrasted by the ELC, which has its annual maximum of PA in December due to its exposure to the NEM (Fig. 3d) and its location adjacent to the Sierra Madre mountains (Fig. 1b), further highlighting the role of mountain ranges in determining the impact of the monsoons on precipitation (Xie et al. 2006; Akasaka et al. 2007; Riley Dellaripa et al. 2020).

The diurnal cycle of light precipitation (0.01–2.5 mm h^{-1}) in MJJAS (Fig. 6) was observed to capture total precipitation quite well in all regions. Considering the importance of light precipitation and the poor performance of satellite precipitation products in detecting lighter precipitation in the Philippines (Jamandre and Narisma 2013; Peralta et al. 2020), this indicates a need for further improvement of satellite retrievals to capture observed precipitation trends in the Philippines. Heavy precipitation (exceeding 2.5 mm h^{-1}) across regions occurred in the morning (8–12 LST) (Figs. 6b; S1c), particularly over the WLC, a feature that will be a topic of future research. Zhuo et al. (2014) observed that peak timing of precipitation varied with intensity, occurring either in the early morning (0–8 LST) and late afternoon (13–16 LST). While Zhuo et al. (2014) attributed the morning peak to monsoonal influence, our observed morning peak of heavy precipitation may be related to a combination of monsoonal influence and daytime heating. However, it is also noted that these heavy precipitation occurrences are very rare as the morning peaks do not appear in the mean PA cycle (Fig. 4a).

Given these findings, questions remain such as seasonal changes in the diurnal cycle in regions of different topography (Fig. 3). Seasonal shifts in the diurnal peak of PA are visible in Fig. 3 and may be examined in future work. A higher resolution model may be able to resolve the migration of precipitation along mountain slopes and the effect of coastal or mountain range curvature on the diurnal cycle, particularly over WLC and ELC. As the influence of monsoons in the CV is likely modulated by mountain ranges to the west and east, other physical mechanisms besides the monsoon may be

responsible for diurnal precipitation patterns in the CV. Furthermore, the observed heavy precipitation over the WLC in the morning should be investigated in more detail. The effect of more complicated topography in Visayas and Mindanao (Fig. 1a) on the diurnal cycle of precipitation is also recommended as topics of future research. Finally, evaluation of satellite-based datasets (Jamandre and Narisma 2013; Peralta et al. 2020) may also be performed with the denser network of stations used in this study.

4.2 Conclusions

Using a spatially dense network of 411 stations across Luzon Island in the Philippines, we present the first attempt of examining the diurnal cycle of precipitation across Luzon. Diurnal characteristics of PA, PI, and PF were described across different seasons of the year from January 2011 to April 2018. PA is the accumulated hourly precipitation divided by the total number of hours, PF is defined as the total number of hours with hourly-averaged precipitation above 0.01 mm h^{-1} divided by the total number of hours, and PI is defined as PA divided by PF. We compared regions of distinct topography such as a valley (CV), a plain (CLP), a west-facing coast (WLC), and an east-facing coast (ELC) to further understand the interaction of local topography with local- and large-scale circulation. As the SWM contributes the most precipitation throughout the year, we focused our analysis primarily on MJJAS.

Results showed that the spatial patterns of PA and PF in MJJAS correspond well to large-scale seasonal/monsoonal flows and generally decreased toward the leeward side of the Philippines relative to the prevailing monsoon such that the west (east) side of Luzon exhibited higher (lower) PA and PF. High values of PA and PF were observed near the Cordillera mountains (Figs. 1 and 2), corroborating previous satellite-based studies (Xin-Xin et al. 2015; Takahashi 2016). High PI values appeared opposite of the direction of monsoon flow.

Dividing Luzon into regions, we observed differences in the diurnal cycles across regions. The ELC showed relatively consistent PA for most of the year with an annual maximum in December (Fig. 3), while other regions experienced large PA values in MJJAS. Such differences were attributed to the effect of nearby mountain ranges on moisture flux (Xie et al. 2006) in combination with seasonal changes in the prevailing wind. In addition to information from previous studies on seasonal precipitation (Akasaka et al. 2007; Park et al. 2011; Pullen et al. 2015), this study found that diurnal precipitation in MJJAS across most regions in Luzon peaked in the late afternoon-early evening with the exception of the ELC, which exhibited scattered peaks throughout the day and a slight peak in the late evening-early morning. Similar peak timings are indicative of the large-scale enhancement of precipitation by the SWM. Diurnal cycles of PI showed much higher variability throughout the day but generally peaked at the same times as PA and PF, which suggests that PI and PF are both important indicators of PA. Furthermore, a shift in precipitation characteristics was observed during the peak of PA, with the first (second) half exhibiting high PI and low PF (low PI and high PF).

The diurnal cycle was found to vary across most regions as a result of nearby mountain ranges. In MJJAS, the WLC showed differing diurnal cycles between its southwest and northeast sections, associated with Zambales and Cordillera mountain ranges, respectively, and their orientation relative to the SWM flows. This contrasts the ELC, which exhibited region-wide peaks scattered throughout the day. The CV experienced most of its precipitation on the west side of the valley while the CLP showed maximum PA values concentrated on the east side of the plain. Both these regions were likely influenced by nearby mountain ranges. One exception to the observed spatiotemporal propagation was the ELC, which exhibited no zonal delay in its PA peaks, explainable by the equal distances of the ELC stations from the nearby mountains.

In terms of graded PA, light precipitation (0.01–2.5 mm h^{-1}) was observed to capture the trends of overall precipitation throughout all four regions, which indicates that observations of the total diurnal cycle can be attributed largely to light precipitation, at least in Luzon, highlighting the importance of understanding this intensity of precipitation. Meanwhile, heavy precipitation appeared between 8–9 LST in the ELC, CV, CLP, and between 8–12 LST in the WLC. As expected, west side regions (i.e., WLC, CLP) contributed majority of precipitation during the SWM season.

Acknowledgements The authors are grateful for the constructive comments from the editor and anonymous reviewers in further improving this manuscript. The authors would like to thank Mr. Emilio Gozo of the Manila Observatory for preparing the Weather Philippines Foundation data set. This research was done during the internship of Miguel Hilario at Tokyo Metropolitan University in 2018 and was supported by the Japan Student Services Organization.

Author Contributions MRAH performed the analysis and prepared the manuscript. LMO, GTN, JM supervised the analysis and provided input for the manuscript.

Compliance with Ethical Standards

Conflict of Interest The authors declare no conflict of interest.

References

Akasaka, I.: Interannual variations in seasonal march of rainfall in the Philippines. Int. J. Climatol. **30**, 1301–1314 (2010). https://doi.org/10.1002/joc.1975

Akasaka, I., Morishima, W., Mikami, T.: Seasonal march and its spatial difference of rainfall in the Philippines. Int. J. Climatol. **27**, 715–725 (2007). https://doi.org/10.1002/joc.1428

Betts, A.K., Jakob, C.: Study of diurnal cycle of convective precipitation over Amazonia using a single column model. J. Geophys. Res. Atmospheres. **107**, ACL 25-1–ACL 25-13 (2002). https://doi.org/10.1029/2002JD002264

Biasutti, M., Yuter, S.E., Burleyson, C.D., Sobel, A.H.: Very high resolution rainfall patterns measured by TRMM precipitation radar: seasonal and diurnal cycles. Clim. Dyn. **39**, 239–258 (2012). https://doi.org/10.1007/s00382-011-1146-6

Cayanan, E.O., Chen, T.-C., Argete, J.C., Yen, M.-C., Nilo, P.D.: The effect of tropical cyclones on southwest monsoon rainfall in the Philippines. J. Meteorol. Soc. Jpn. **89A**, 123–139 (2011). https://doi.org/10.2151/jmsj.2011-A08

Chang, C.-P., Wang, Z., McBride, J., Liu, C.-H.: Annual cycle of Southeast Asia—maritime continent rainfall and the asymmetric monsoon transition. J. Clim. **18**, 287–301 (2005). https://doi.org/10.1175/JCLI-3257.1

Chen, F.-W., Liu, C.-W.: Estimation of the spatial rainfall distribution using inverse distance weighting (IDW) in the middle of Taiwan. Paddy Water Environ. **10**, 209–222 (2012). https://doi.org/10.1007/s10333-012-0319-1

Coronas, J.: The Climate and Weather of the Philippines, 1903–1918. Bureau of Printing, Manila, Philippines (1920)

Cruz, F.T., Narisma, G.T., Villafuerte, M.Q., Cheng Chua, K.U., Olaguera, L.M.: A climatological analysis of the southwest monsoon rainfall in the Philippines. Atmospheric Res. **122**, 609–616 (2013). https://doi.org/10.1016/j.atmosres.2012.06.010

Dai, A.: Global precipitation and thunderstorm frequencies. Part I: seasonal and interannual variations. J. Clim. **14**, 20 (2001a)

Dai, A.: Global precipitation and thunderstorm frequencies. Part II: diurnal variations. J. Clim. **14**, 17 (2001b)

Dai, A., Lin, X., Hsu, K.-L.: The frequency, intensity, and diurnal cycle of precipitation in surface and satellite observations over low- and mid-latitudes. Clim. Dyn. **29**, 727–744 (2007). https://doi.org/10.1007/s00382-007-0260-y

DeMott, C.A., Randall, D.A., Khairoutdinov, M.: Convective precipitation variability as a tool for general circulation model analysis. J. Clim. **20**, 91–112 (2007). https://doi.org/10.1175/JCLI3991.1

Flores, J.F., Balagot, V.F.: Climate of the Philippines. World Surv. Climatol. **8**, 159–213 (1969)

Fujibe, F.: Diurnal variation in the frequency of heavy precipitation in Japan. J. Meteorol. Soc. Jpn. Ser II. **77**, 1137–1149 (1999). https://doi.org/10.2151/jmsj1965.77.6_1137

Hersbach, H., Bell, W., Berrisford, P., Horányi, A., J., M.-S., Nicolas, J., Radu, R., Schepers, D., Simmons, A., Soci, C., Dee, D., Dee, D.: Global reanalysis: goodbye ERA-Interim, hello ERA5. ECMWF Newsl. **159**, 17–24 (2019). https://doi.org/10.21957/vf291hehd7

Hirose, M.: Spatial and diurnal variation of precipitation systems over Asia observed by the TRMM precipitation radar. J. Geophys. Res. **110**, D05106 (2005). https://doi.org/10.1029/2004JD004815

Jamandre, C.A., Narisma, G.T.: Spatio-temporal validation of satellite-based rainfall estimates in the Philippines. Atmospheric Res. **122**, 599–608 (2013). https://doi.org/10.1016/j.atmosres.2012.06.024

Johnson, R.H.: Diurnal cycle of monsoon convection. In: In: Chang, C.-P., Ding, Y., Lau, N.-C., Johnson, R.H., Wang, B., and Yasunari, T. (eds.) World Scientific Series on Asia-Pacific Weather and Climate, pp. 257–276. World Scientific (2011)

Kubota, H., Shirooka, R., Matsumoto, J., Cayanan, E.O., Hilario, F.D.: Tropical cyclone influence on the long-term variability of Philippine summer monsoon onset. Prog. Earth Planet. Sci. **4**, 27 (2017). https://doi.org/10.1186/s40645-017-0138-5

Maggioni, V., Meyers, P.C., Robinson, M.D.: A review of merged high-resolution satellite precipitation product accuracy during the Tropical Rainfall Measuring Mission (TRMM) era. J. Hydrometeorol. **17**, 1101–1117 (2016). https://doi.org/10.1175/JHM-D-15-0190.1

Mahmud, M.R., Hashim, M., Reba, M.N.M.: How effective is the new generation of GPM satellite precipitation in characterizing the rainfall variability over Malaysia? Asia-Pac. J. Atmospheric Sci. **53**, 375–384 (2017). https://doi.org/10.1007/s13143-017-0042-3

Matsumoto, J., Olaguera, L.M.P., Nguyen-Le, D., Kubota, H., Villafuerte, M.Q.: Climatological seasonal changes of wind and rainfall in the Philippines. Int. J. Climatol. joc.6492 (2020). https://doi.org/10.1002/joc.6492

Minamide, M., Yoshimura, K.: Orographic effect on the precipitation with typhoon Washi in the Mindanao Island of the Philippines. SOLA. **10**, 67–71 (2014). https://doi.org/10.2151/sola.2014-014

Mori, S., Jun-Ichi, H., Tauhid, Y.I., Yamanaka, M.D., Okamoto, N., Murata, F., Sakurai, N., Hashiguchi, H., Sribimawati, T.: Diurnal Land–Sea rainfall peak migration over Sumatera Island, Indonesian maritime continent, observed by TRMM satellite and intensive Rawinsonde soundings. Mon. Weather Rev. **132**, 19 (2004)

Moron, V., Lucero, A., Hilario, F., Lyon, B., Robertson, A.W., DeWitt, D.: Spatio-temporal variability and predictability of summer monsoon onset over the Philippines. Clim. Dyn. **33**, 1159–1177 (2009). https://doi.org/10.1007/s00382-008-0520-5

Ohsawa, T., Ueda, H., Hayashi, T., Watanabe, A., Matsumoto, J.: Diurnal variations of convective activity and rainfall in tropical Asia. J. Meteorol. Soc. Jpn. Ser II. **79**, 333–352 (2001). https://doi.org/10.2151/jmsj.79.333

Oki, T., Musiake, K.: Seasonal change of the diurnal cycle of precipitation over Japan and Malaysia. J. Appl. Meteorol. **33**, 1445–1463 (1994). https://doi.org/10.1175/1520-0450(1994)033<1445:SCOTDC>2.0.CO;2

Olaguera, L.M.P., Matsumoto, J.: A climatological study of the wet and dry conditions in the pre-summer monsoon season of the Philippines. Int. J. Climatol. **40**(9), 4203–4217 (2019). https://doi.org/10.1002/joc.6452

Olaguera, L., Matsumoto, J., Kubota, H., Inoue, T., Cayanan, E., Hilario, F.: Abrupt climate shift in the mature rainy season of the Philippines in the mid-1990s. Atmosphere. **9**, 350 (2018a). https://doi.org/10.3390/atmos9090350

Olaguera, L.M., Matsumoto, J., Kubota, H., Inoue, T., Cayanan, E.O., Hilario, F.D.: Interdecadal shifts in the winter monsoon rainfall of the Philippines. Atmosphere. **9**, 464 (2018b). https://doi.org/10.3390/atmos9120464

Park, M.-S., Ho, C.-H., Kim, J., Elsberry, R.L.: Diurnal circulations and their multi-scale interaction leading to rainfall over the South China Sea upstream of the Philippines during intraseasonal monsoon westerly wind bursts. Clim. Dyn. **37**, 1483–1499 (2011). https://doi.org/10.1007/s00382-010-0922-z

Peralta, J.C.A.C., Narisma, G.T.T., Cruz, F.A.T.: Validation of satellite and ground station-based high-resolution rainfall gridded datasets over the Philippines. J. Hydrometeorol. **21**(7), 1571–1587 (2020). https://doi.org/10.1175/JHM-D-19-0276.1

Pullen, J., Gordon, A.L., Flatau, M., Doyle, J.D., Villanoy, C., Cabrera, O.: Multiscale influences on extreme winter rainfall in the Philippines. J. Geophys. Res. Atmospheres. **120**, 3292–3309 (2015). https://doi.org/10.1002/2014JD022645

Qian, J.-H.: Why precipitation is mostly concentrated over islands in the maritime continent. J. Atmos. Sci. **65**, 1428–1441 (2008). https://doi.org/10.1175/2007JAS2422.1

Qian, T., Dai, A., Trenberth, K.E., Oleson, K.W.: Simulation of global land surface conditions from 1948 to 2004. Part I: forcing data and evaluations. J. Hydrometeorol. **7**, 953–975 (2006). https://doi.org/10.1175/JHM540.1

Qian, J.-H., Robertson, A.W., Moron, V.: Interactions among ENSO, the monsoon, and diurnal cycle in rainfall variability over Java, Indonesia. J. Atmospheric Sci. **67**, 3509–3524 (2010). https://doi.org/10.1175/2010JAS3348.1

Reiter, E., Tang, M.: Plateau effects on diurnal circulation patterns. Mon. Weather Rev. **112**, 638–651 (1984). https://doi.org/10.1175/1520-0493(1984)112<0638:PEODCP>2.0.CO;2

Riley Dellaripa, E.M., Maloney, E.D., Toms, B.A., Saleeby, S.M., van den Heever, S.C.: Topographic effects on the Luzon diurnal cycle during the BSISO. J. Atmos. Sci. **77**, 3–30 (2020). https://doi.org/10.1175/JAS-D-19-0046.1

Saito, K., Keenan, T., Holland, G., Puri, K.: Numerical simulation of the diurnal evolution of Tropical Island convection over the maritime continent. Mon. Weather Rev. **129**, 23 (2001)

Sakurai, N., Kawashima, M., Fujiyoshi, Y., Hashiguchi, H., Shimomai, T., Mori, S., Jun-Ichi, H., Murata, F., Yamanaka, M.D., Tauhid, Y.I., Sribimawati, T., Suhardi, B.: Internal structures of migratory cloud systems with diurnal cycle over Sumatera Island during CPEA-I campaign. J. Meteorol. Soc. Jpn. **87**, 157–170 (2009). https://doi.org/10.2151/jmsj.87.157

Sakurai, N., Mori, S., Kawashima, M., Fujiyoshi, Y., Hamada, J.-I., Shimizu, S., Fudeyasu, H., Tabata, Y., Harjupa, W., Hashiguchi, H., Yamanaka, M.D., Matsumoto, J., Emrizal, Syamsudin, F.: Migration process and 3D wind field of precipitation systems associated with a diurnal cycle in West Sumatera: dual doppler radar analysis during the HARIMAU2006 campaign. J. Meteorol. Soc. Jpn. **89**, 341–361 (2011). https://doi.org/10.2151/jmsj.2011-404

Sakurai, N., Murata, F., Yamanaka, M.D., Mori, S., Hamada, J.-I., Hashiguchi, H., Tauhid, Y.I., Sribimawati, T., Suhardi, B.: Diurnal cycle of cloud system migration over Sumatera Island. J. Meteorol. Soc. Jpn. **83**, 835–850 (2005). https://doi.org/10.2151/jmsj.83.835

Satomura, T.: Diurnal variation of precipitation over the Indo-China peninsula. J. Meteorol. Soc. Jpn. **78**, 461–475 (2000). https://doi.org/10.2151/jmsj1965.78.4_461

Shibagaki, Y., Shimomai, T., Kozu, T., Mori, S., Fujiyoshi, Y., Hashiguchi, H., Yamamoto, M.K., Fukao, S., Yamanaka, M.D.: Multiscale aspects of convective systems associated with an Intraseasonal oscillation over the Indonesian maritime continent. Mon. Weather Rev. **134**, 1682–1696 (2006). https://doi.org/10.1175/MWR3152.1

Sun, Y., Solomon, S., Dai, A., Portmann, R.W.: How often does it rain? J. Clim. **19**, 916–934 (2006). https://doi.org/10.1175/JCLI3672.1

Sun, Y., Solomon, S., Dai, A., Portmann, R.W.: How often will it rain? J. Clim. **20**, 4801–4818 (2007). https://doi.org/10.1175/JCLI4263.1

Takahashi, H.G.: Seasonal changes in diurnal rainfall cycle over and around the Indochina peninsula observed by TRMM-PR. Adv. Geosci. **25**, 23–28 (2010). https://doi.org/10.5194/adgeo-25-23-2010

Takahashi, H.G.: Seasonal and diurnal variations in rainfall characteristics over the tropical Asian monsoon region using TRMM-PR data. SOLA. **12A**, 22–27 (2016). https://doi.org/10.2151/sola.12A-005

Takahashi, H.G., Polcher, J.: Weakening of rainfall intensity on wet soils over the wet Asian monsoon region using a high-resolution regional climate model. Prog. Earth Planet. Sci. **6**, 26 (2019). https://doi.org/10.1186/s40645-019-0272-3

Trenberth, K.E., Dai, A., Rasmussen, R.M., Parsons, D.B.: The changing character of precipitation. Bull. Amer. Meteor. Soc. **84**, 1205–1218 (2003). https://doi.org/10.1175/BAMS-84-9-1205

Tsujimoto, K., Ohta, T., Aida, K., Tamakawa, K., So Im, M.: Diurnal pattern of rainfall in Cambodia: its regional characteristics and local circulation. Prog. Earth Planet. Sci. **5**, 39 (2018). https://doi.org/10.1186/s40645-018-0192-7

Villafuerte, M.Q., Matsumoto, J., Akasaka, I., Takahashi, H.G., Kubota, H., Cinco, T.A.: Long-term trends and variability of rainfall extremes in the Philippines. Atmospheric Res. **137**, 1–13 (2014). https://doi.org/10.1016/j.atmosres.2013.09.021

Xie, S.-P., Xu, H., Saji, N.H., Wang, Y., Liu, W.T.: Role of narrow mountains in large-scale organization of Asian monsoon convection*. J. Clim. **19**, 3420–3429 (2006). https://doi.org/10.1175/JCLI3777.1

Xin-Xin, Z., Xun-Qiang, B., Xiang-Hui, K.: Observed diurnal cycle of summer precipitation over South Asia and East Asia based on CMORPH and TRMM satellite data. Atmospheric Ocean. Sci. Lett. **8**, 201–207 (2015). https://doi.org/10.1080/16742834.2015.11447260

Yamanaka, M.D.: Physical climatology of Indonesian maritime continent: an outline to comprehend observational studies. Atmospheric Res. **178–179**, 231–259 (2016). https://doi.org/10.1016/j.atmosres.2016.03.017

Yamanaka, M.D., Ogino, S.-Y., Wu, P.-M., Jun-Ichi, H., Mori, S., Matsumoto, J., Syamsudin, F.: Maritime continent coastlines controlling Earth's climate. Prog. Earth Planet. Sci. **5**, 21 (2018). https://doi.org/10.1186/s40645-018-0174-9

Yang, G.-Y., Slingo, J.: The diurnal cycle in the tropics. Mon. Weather Rev. **129**, 18 (2001)

Yin, S., Chen, D., Xie, Y.: Diurnal variations of precipitation during the warm season over China. Int. J. Climatol. **29**, 1154–1170 (2009). https://doi.org/10.1002/joc.1758

Yokoi, S., Satomura, T., Matsumoto, J.: Climatological characteristics of the Intraseasonal variation of precipitation over the Indochina peninsula. J. Clim. **20**, 5301–5315 (2007). https://doi.org/10.1175/2007JCLI1357.1

Yu, R., Zhou, T., Xiong, A., Zhu, Y., Li, J.: Diurnal variations of summer precipitation over contiguous China. Geophys. Res. Lett. **34**, L01704 (2007). https://doi.org/10.1029/2006GL028129

Yuan, W., Yu, R., Chen, H., Li, J., Zhang, M.: Subseasonal characteristics of diurnal variation in summer monsoon rainfall over Central Eastern China. J. Clim. **23**, 6684–6695 (2010). https://doi.org/10.1175/2010JCLI3805.1

Zhang, W., Huang, A., Zhou, Y., Yang, B., Fang, D., Zhang, L., Wu, Y.: Diurnal cycle of precipitation over Fujian Province during the pre-summer rainy season in southern China. Theor. Appl. Climatol. **130**, 993–1006 (2017). https://doi.org/10.1007/s00704-016-1927-2

Zhou, T., Yu, R., Chen, H., Dai, A., Pan, Y.: Summer precipitation frequency, intensity, and diurnal cycle over China: a comparison of satellite data with rain gauge observations. J. Clim. **21**, 3997–4010 (2008). https://doi.org/10.1175/2008JCLI2028.1

Zhuo, H., Zhao, P., Zhou, T.: Diurnal cycle of summer rainfall in Shandong of eastern China. Int. J. Climatol. **34**, 742–750 (2014). https://doi.org/10.1002/joc.3718